physica status solidi a

www.pss-a.com

applications and materials science

Temperature dependence of the *I–V* characteristics of Ni/Au Schottky contacts to AlGaN/GaN heterostructures grown on Si substrates

G. Greco*,1, S. Di Franco1, F. Iucolano2, F. Giannazzo1, and F. Roccaforte1

[1] CNR-IMM, Strada VIII, n. 5 − Zona Industriale, 95121 Catania, Italy
[2] STMicroelectronics, Stradale Primosole 50, 95121 Catania, Italy

* Corresponding author: e-mail giuseppe.greco@imm.cnr.it, Phone: +39 0955968243, Fax: +3909559680211

The forward current–voltage (*I–V*) characteristics of Ni/Au Schottky contacts on AlGaN/GaN heterostructures have been studied in this work. The electrical characteristics exhibited a strongly non-ideal behavior that could not be described by the thermionic emission theory. Hence, we used a "two diodes model," considering both the presence of the Ni/AlGaN barrier and of a second barrier height at the AlGaN/GaN hetero-junction. Capacitance–voltage (*C–V*) measurements enabled us to experimentally determine the properties of the two dimensional electron gas (2DEG) and, hence, of the second barrier at the AlGaN/GaN interface. Following this approach, the anomalous *I–V* curves could be explained. Moreover, the value of the barrier height at zero-electric field (flat-band barrier height) was introduced and determined with this procedure, and resulted in a good agreement with literature data based on photoemission measurements. This approach provides a valid procedure for an accurate determination of the barrier height in AlGaN/GaN heterostructures, and the results can have useful implications for the fabrication of AlGaN/GaN HEMTs devices.

1 Introduction The presence of a two dimensional electron gas (2DEG) [1] is an important characteristic of strained AlGaN/GaN heterostructures, which makes these systems suitable for the fabrication of high electron mobility transistors (HEMTs). In particular, the high mobility of the 2DEG permits the operation of HEMT devices at high frequencies ($f_\mathrm{T} > 200\,\mathrm{GHz}$) in low voltages applications [2]. Moreover, owing to the wide band gap and high electric field strength of GaN and related $Al_xGa_{1-x}N$ alloys, these transistors can work at high breakdown voltages (600–1200 V) with specific on-resistance values of few mΩ-cm^2 [3]. Hence, AlGaN/GaN heterostructures are excellent candidates to cover a wide range of future RF-power applications with an improved energy efficiency [4].

Contextually, understanding the transport mechanisms at metal/AlGaN interfaces is a key topic, since Schottky barriers are essential bricks in the operation of these devices.

As a matter of fact, the AlGaN/GaN HEMTs functionality can be strongly affected by the gate leakage current, or by the degradation phenomena of the Schottky barrier occurring under current stress [5, 6].

Many works on Schottky barriers on n-type GaN have been reported in the last 20 years [7–12]. The current transport mechanisms at metal/GaN interfaces has been often described invoking the thermionic emission (TE) or thermionic field emission (TFE) theories [13–18]. In this context, also the impact of surface processing steps [19, 20] or post-annealing treatments [21], as well as the role of the defects present in the material [22–24], have been investigated.

On the other hand, the number of reports on Schottky contacts on AlGaN/GaN heterostructures increased parallel to the interest towards HEMTs devices in the very last years. For AlGaN/GaN HEMTs, metals with a high work-function

are preferred to obtain a high barrier height and to reduce the leakage current at the gate electrode [25, 26]. In these systems, the temperature dependence of the I–V characteristics of Schottky contacts has been described either using TE [27] or tunneling-based mechanisms [14]. In particular, it has been pointed out that the occurrence of carrier the tunneling mechanisms (TFE, FE, Poole-Frenkel,...) at metal/semiconductor interfaces can be enhanced in the presence of a high density of material defects (e.g., dislocations) in the heterostructures [28–30].

Obviously, AlGaN/GaN heterostructures are complex systems, in which the presence of a potential well and a 2DEG at the heterojunction can have an influence on the properties of a metal/semiconductor Schottky barrier, formed at the surface of the AlGaN layer. For that reason, some works recently proposed alternative models for Schottky barriers on AlGaN/GaN heterostructures, to consider the effects of polarization charges and the presence of the 2DEG [31, 32].

Chen et al. [33] had proposed a "two diodes model" for the AlGaAs/GaAs system, which considered a first barrier at the metal/AlGaAs interface and a second one at the AlGaAs/GaAs heterojunction. This model was recently adapted by Lv et al. [34] to describe the characteristics of AlGaN/GaN Schottky diodes measured at room temperature. However, in these papers the temperature dependence of the characteristics was not analyzed. Moreover, these works did not consider the possible influence of the metal/semiconductor contact (whose properties depends on the experimental conditions) on the properties of the 2DEG.

In this paper, the forward current–voltage characteristics of Ni/Au Schottky contacts on AlGaN/GaN heterostructures has been studied and the results were explained by means of a "two diodes model." Our approach included the experimental determination of the 2DEG properties by C–V measurements. In this way, the influence of the metal/semiconductor interface on the properties of the underlying 2DEG was also taken into account. This approach allowed us to explain the non-ideal behavior of the electrical characteristics and led to a correct determination of the Ni/AlGaN barrier height, introducing the concept of flat-band barrier height. Our electrical results were corroborated by the comparison with literature data obtained by photoemission measurements of the barrier height.

2 Experimental AlGaN/GaN heterostructures grown on silicon substrates were used in this work. The Al-concentration in the 20 nm thick AlGaN barrier layer was 24% ($x_{Al} = 0.24$). On this material, lateral Schottky diodes were fabricated in order to study the electrical properties of a Ni/AlGaN barrier. For this purpose, Ohmic contacts were first created by a Ti/Al/Ni/Au (15/200/50/50 nm) multilayer annealed at 850 °C [35]. Thereafter, Ni/Au circular Schottky contacts of area $7 \times 10^{-4}\,cm^2$ have been defined by lift-off and subjected to a post deposition rapid annealing at 400 °C in Ar atmosphere for 60 s in a Jipelec JetFirst furnace, in order to improve the metal/semiconductor

interface quality and to reduce the series resistance [36]. The electrical characterization of the diodes has been performed on a Karl Suss Microtec probe station, equipped with HP 4156B and Agilent B1505. In particular, the forward current density vs voltage (J–V) characteristics of the diodes have been acquired in the temperature range 25–150 °C, to get information on the barrier height and the transport mechanisms. On the other hand, capacitance-voltage (C–V) measurements allowed to determine the experimental value of the sheet carrier concentration, n_s, in the 2DEG.

3 Results and discussion On n-type GaN layers (i.e., in the absence of an heterostructure), the J–V characteristics of Schottky contacts are frequently described using the TE theory [37]:

$$J = A^* T^2 e^{-\frac{q\Phi_B}{kT}} \left(e^{\frac{qV}{nkT}} - 1 \right) \quad (1)$$

where A^* is the Richardson's constant, k is the Boltzmann constant, and n and Φ_B are the ideality factor and the Schottky barrier height, respectively.

The forward J–V curves, acquired at different measurement temperatures on our Ni/Au Schottky diodes on AlGaN/GaN heterostructures, are reported in a semilogarithmic plot in Fig. 1. Clearly, these characteristics show a strong deviation from the ideal behavior, as can be seen from the occurrence of two regions having different slopes (indicated as Reg. I and Reg. II).

Using the TE theory (Eq. 1), the values of the ideality factor n and of the barrier height Φ_B were calculated at each temperature, from a linear fit of the J–V curves in the Reg. I ($0.6\,V < V < 1.1\,V$). These values are reported in Table 1. As can be seen, the experimental values of the ideality factor are rather high ($n > 2$), while the values of the barrier height Φ_B lie in the range 0.77–1.12 eV. The high ideality factor
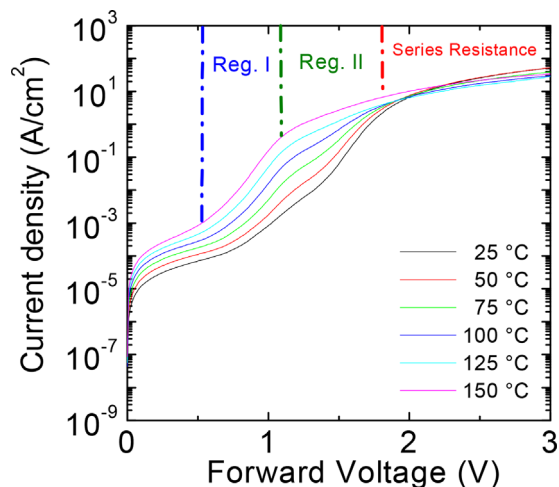

Figure 1 Temperature dependence of the forward I–V characteristics of Ni/Au Schottky contacts on AlGaN/GaN heterostructures. The occurrence of two regions with different slopes is highlighted.

Table 1 Experimental values of the ideality factor n and of the Schottky barrier height $\Phi_{B(TE)}$ determined by the standard thermionic emission (TE) theory, that is, applying to the Eq. 1 to the Reg. I of the J–V curves of our Ni/AlGaN/GaN Schottky diodes.

measurement temperature T (°C)	ideality factor n	barrier height $\Phi_{B(TE)}$ (eV)
25	4.74	0.77
50	3.70	0.86
75	2.99	0.95
100	2.50	1.02
125	2.24	1.07
150	2.05	1.12

measured at room temperature suggests that the mechanism of current transport is different from a standard TE model. Moreover, both the ideality factor n and the Schottky barrier height Φ_B exhibit a strong dependence of the temperature. Different factors can be responsible for the non-ideal behavior of a Schottky barrier, such as the image force lowering effect, the presence of an interfacial layer, the occurrence of carrier tunneling through the barrier, etc [38]. The barrier lowering related to the image force effect, shows only a slight deviation of the ideality factor from the unity. Moreover, it typically leads to a weak increase of the ideality factor with the temperature [39]. Yan et al. [30] correlated a slight dependence of the ideality factor on the temperature with a combination of different mechanisms. On the other hand, Arslan et al. [29] justified the non-ideal behavior of the diode with the high dislocation density in the material, fitting the temperature dependence of the ideality factor with the TFE model with a characteristic energy $E_{00} = 85.7$ meV. In our case, the strong dependence of the ideality factor on the measurement temperature cannot be fitted by applying the TFE model, considering different values of the fitting parameters E_{00}.

Instead, an explanation of the temperature behavior of the ideality factor and of the barrier height can be given using the model proposed by Tung [40]. In fact, a strong temperature dependence of n and Φ_B is typically the macroscopic manifestation of a lateral inhomogeneity of the Schottky barrier at a nanoscale level. In particular, according to Tung's model [40], an "inhomogeneous" Schottky barrier can be described by a distribution of regions with a low-barrier embedded in a background with a uniform ideal high-barrier. Hence, at high temperatures the carriers will have enough energy to overcome the highest ideal barrier by a TE emission, and consequently, the measured ideality factor will decrease toward the unity. On the other side, at low temperatures, the carriers will have sufficient energy only to overcome the regions at lower barrier. Then, strong deviation from the ideality and a lower experimental value of Φ_B are measured. A similar trend has been already observed in other wide band gap semiconductors [41, 42]. Clearly, the standard TE theory is not the most suitable model to describe the carrier transport mechanisms in our Ni/AlGaN interface.

A more accurate description of our system was given by appropriately adapting the "two diodes model" for heterostructures [33, 34]. Following this approach, the metal/AlGaN/GaN system can be described as two diodes in series, in a "back-to-back" configuration. Namely, the equivalent circuit is formed by a first diode (D_1) in forward bias, given by the metal/AlGaN interface, and a second (D_2) in reverse bias, represented by the barrier at the AlGaN/GaN interface. Figure 2 reports a schematic of the conduction band diagram at zero-bias of the "two diodes model," with the equivalent circuit. In this scheme, Φ_{B1} is the barrier height formed at the metal/AlGaN interface (diode D_1), while $\Phi_{B2}(0)$ is zero-bias value of the second barrier (diode D_2).

When such a system is polarized, the total external applied bias V, will partially drop on the two diodes, that is, $V = V_1 + V_2$. Figure 3 reports, as an example, the forward J–V curve acquired at 100 °C on a Ni/AlGaN/GaN Schottky diode. For low values of the applied bias V (Reg. I), the applied voltage will drop entirely on the first barrier and the J–V curve will be determined by the conduction of the diode D_1. Then, by increasing the applied bias, the semiconductor Fermi level will be raised, part V_2 of the bias will drop on the second reversed biased diode D_2 and the contribution to the conduction will appear as a second slope in the J–V curve (Reg. II). Finally, with a further increase of the applied voltage (e.g., >2 V) the series resistance will become dominant.

The forward current density for the diode D_1 (i.e., the current in the Reg. I) can be written as:

$$J_{D1} = A^* T^2 e^{-\frac{q\Phi_{B1}(0)}{kT}} e^{\frac{qV_1}{n_1 kT}} = J_{S1} e^{\frac{qV_1}{n_1 kT}} \qquad (2)$$

where V_1 is the voltage drop across diode D_1, n_1 is the ideality factor of diode D_1 and $\Phi_{B1}(0)$ is the zero-bias barrier
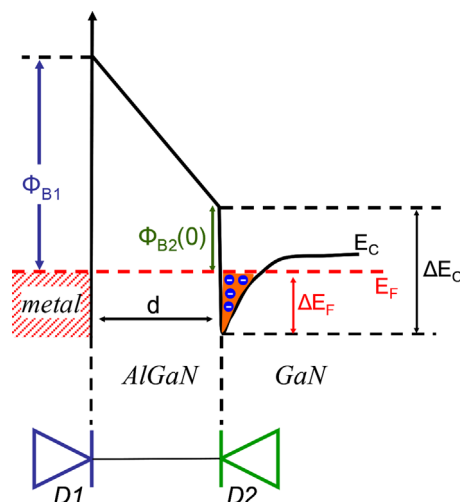

Figure 2 Schematic representation of the zero-bias conduction band diagram of the AlGaN/GaN heterostructure and the equivalent circuit describing the "two diodes model".
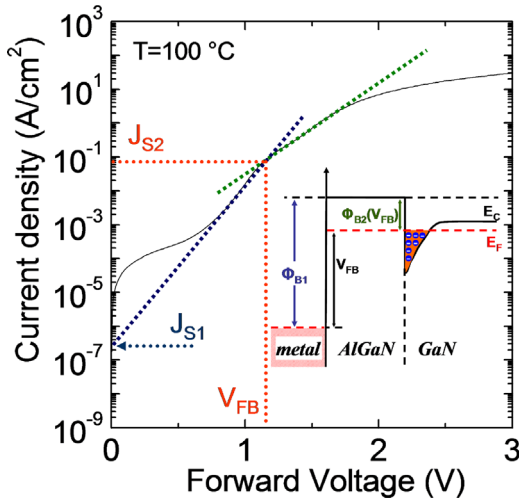
Figure 3 Example of a forward J–V characteristic acquired at $100\,^\circ$C in Ni/Au Schottky contacts on AlGaN/GaN heterostructures. The dashed lines represent the linear fits carried out in the two regions to extract the saturation currents of the two diodes. The inset shows the band diagram at the flat-band condition.

height. In Eq. 2, J_{S1} is the saturation current density of the diode, which can be extrapolated by a linear fit of the J–V curves, as schematically indicated by the dashed line in the example of Fig. 3.

Similarly, the current density for the diode D_2 can be expressed in the form:

$$J_{D2} = A^* T^2 e^{-\frac{q\Phi_{B2}(0)}{kT}} e^{\frac{qV_2}{n_2 kT}} = J_{S2} e^{\frac{qV_2}{n_2 kT}} \qquad (3)$$

where V_2 is the voltage drop across diode D_2, n_2 is the ideality factor of diode D_2 and $\Phi_{B2}(0)$ is the zero-bias barrier height. The derivation of Eq. 3 is given in Appendix I.

The saturation current density J_{S2} can be determined by a linear fit of the experimental J–V curves in the Reg. II. However, due to the fact that only a part of the applied external bias drops on the diode D_2, that is V_2, in order to correctly extrapolate J_{S2} one has to consider the intersection of the linear fit of the diode D_2 with that of the diode D_1, as graphically shown in the example in Fig. 3. Noteworthy, the abscissa of the intersection point of the two fits corresponds to the absence of voltage drops on the diode D_2, that is $V_2 = 0$, where the systems is in the flat-band condition (V_{FB}). The inset in Fig. 3 depicts the conduction band diagram of the system in the flat-band condition, that is, where the conduction of the second barrier sets in.

In order to accurately determine the values of the two barriers of the AlGaN/GaN system from Eqs. 2 and 3, the knowledge of the effective Richardson's constant A^* is required. This parameter is known to be strongly dependent on the metal/semiconductor interface homogeneity [24, 43].

However, combining the expressions of the saturation current densities J_{S1} and J_{S2} (Eqs. 2 and 3) results in:

$$\Phi_{B1}(0) = \Phi_{B2}(0) + \frac{kT}{q}\ln\left(\frac{J_{S2}}{J_{S1}}\right) \qquad (4)$$

which correlates the zero-bias values of the two barriers and does not explicitly contain the Richardson's constant A^*.

Now, in order to determine $\Phi_{B1}(0)$ from Eq. 4, besides J_{S1} and J_{S2} that can be extrapolated from the linear fits of the J–V curves as described before, also the value of $\Phi_{B2}(0)$ must be known.

The zero-bias barrier height $\Phi_{B2}(0)$ depends on the heterostructure properties, as it is given by the energy difference:

$$\Phi_{B2}(0) = \Delta E_C - \Delta E_F \qquad (5)$$

where ΔE_C is the band gap discontinuity between AlGaN and GaN at the interface, and ΔE_F is the position of the Fermi level with respect to the GaN conduction band at the interface (see Fig. 2).

For our heterostructure, a value of the band gap discontinuity of $\Delta E_C = 0.32$ eV has been assumed from the relation $\Delta E_C = 0.7\left[E_{gap}(x_{Al}) - E_{gap}(0)\right]$ between the GaN band gap $E_{gap}(0)$ and the AlGaN band gap $E_{gap}(x_{Al})$ for $x_{Al} = 0.24$, [1, 44]

To calculate ΔE_F, a straightforward approach based on the experimental determination of the 2DEG properties is proposed. In particular, ΔE_F can be experimentally determined by C–V measurements carried out on the Schottky diode. In fact, by integrating the C–V curves it is possible to extract the experimental sheet carrier concentration n_S of the 2DEG as a function of the applied voltage, as shown in Fig. 4. Then, the value of ΔE_F can be determined inserting the experimental value of n_S in the relation [1]:

$$\Delta E_F = \frac{\pi\hbar^2}{qm^*}n_S + \frac{1}{q}\left(\frac{9\pi\hbar q^2}{8\varepsilon_0\varepsilon_{AlGaN}\sqrt{8m^*}}\right)^{2/3}(n_S)^{2/3} \qquad (6)$$
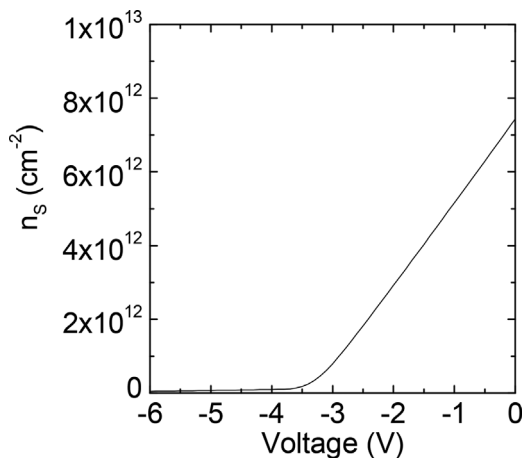

Figure 4 Sheet carrier density (n_S) of the 2DEG as a function of the applied voltage, determined by C–V measurements.

Original
Paper

Phys. Status Solidi A (2017)   (5 of 8) 1600764

where $\hbar$ is the reduced Pank's constant, ε_0 is the vacuum permittivity, ε_{AlGaN} and m^* are the dielectric constant and the effective electron mass of the AlGaN, respectively.

Hence, considering the value of n_S at $V = 0$ determined by the C–V analysis ($7.43 \times 10^{12}\,\text{cm}^{-2}$) yields a $\Delta E_F = 0.036\,\text{eV}$, which when inserted into Eq. 5 allowed us to determine an experimental value of $\Phi_{B2}(0) = 0.28\,\text{eV}$ for the heterostructure analyzed in this work.

Finally, once the values of J_{S1}, J_{S2}, and $\Phi_{B2}(0)$ have been determined, the experimental value of $\Phi_{B1}(0)$ can be calculated at each temperature using Eq. 4.

In Fig. 5, the temperature dependence of the barrier height calculated with the "two diodes model" $\Phi_{B1}(0)$ is reported, together with the values of the barrier extracted with standard TE model $\Phi_{B(TE)}$. As can be seen, $\Phi_{B1}(0)$ results lower than $\Phi_{B(TE)}$, and both parameters are significantly dependent on the temperature. In fact, the zero-bias barrier height, extracted by current–voltage measurements, is influenced by metal/semiconductor interface inhomogeneities, thus leading to the observed dependence of the barrier height on the temperature. For that reason, the values of $\Phi_{B(TE)}$ and $\Phi_{B1}(0)$ are lower with respect to the theoretical Schottky–Mott prediction.

Then, in order to describe more accurately the metal/semiconductor barrier, it is useful to introduce the flat-band Schottky barrier height Φ_{FB}, that is, the barrier height at zero electrical field.

In a metal/semiconductor interface, the flat-band Schottky barrier height Φ_{FB}, defined as the barrier height calculated at the flat band voltage, can be correlated to the zero-bias barrier height $\Phi_B(0)$ through the relation [45]:

$$\Phi_{FB} = n\,\Phi_B(0) - (n-1)\,V_n \tag{7}$$

where V_n is distance of the Fermi level from the conduction band edge:

$$V_n = \frac{kT}{q}\ln\frac{N_C}{N_D} \tag{8}$$

where N_C is the effective conduction-band density of states and N_D is the n-type semiconductor donor density.

Similarly, in an AlGaN/GaN heterostructure, the flat-band voltage barrier height Φ_{FB} can be written as:

$$\Phi_{FB} = n\,\Phi_{B1}(0) - (n-1)\,\Phi_{B2}(0) \tag{9}$$

Details on the derivation of Eqs. 7 and 9 are given in Appendix II.

From Eq. 9, it was possible to calculate the value of Φ_{FB}, considering the temperature dependent values of the zero-bias Ni/AlGaN barrier $\Phi_{B1}(0)$, the temperature dependence of the ideality factor, and the experimental $\Phi_{B2}(0)$. As can be seen in Fig. 5, an almost temperature independent value of the flat-band barrier height of about 1.40 eV was found with this procedure. Moreover, the obtained Φ_{FB} is in good agreement with the theoretical value of 1.44 eV predicted by the Schottky–Mott relation $\Phi_{FB} = \Phi_m - \chi_{AlGaN}$, where Φ_m is the metal work function (5.1 eV in case of the Ni) and χ_{AlGaN} is the AlGaN electron affinity (3.68 eV for an Al-concentration of 24%).

It is worth noting that in a metal/semiconductor contact the value of the experimental Schottky barrier height depends on the measurement technique [46]. Among the used techniques, photoemission measurements are considered to give the most reliable values of the barrier height in
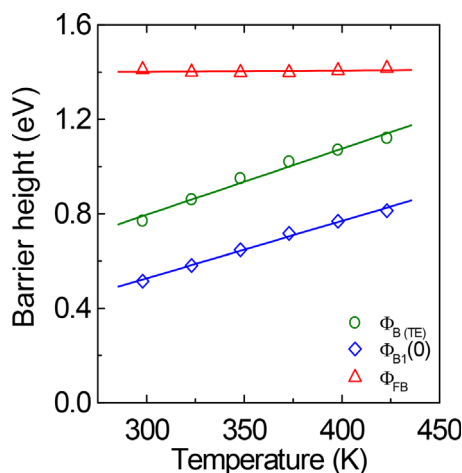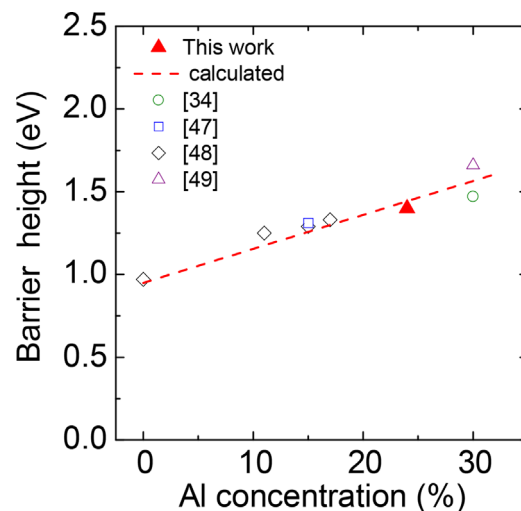
Figure 5 Temperature dependence of the zero-bias barrier height Φ_B calculated by standard TE model ($\Phi_{B(TE)}$) and by the "two diodes model" ($\Phi_{B1}(0)$). The temperature dependence of the flat-band barrier height (Φ_{FB}) is also reported. The continuous lines are to guide the eye only.

Figure 6 Collection of literature data of the Schottky barrier height for Ni/Au Schottky contacts to AlGaN/GaN heterostructures as a function of the Al-concentration, determined by photoemission measurements. The experimental value of the flat band barrier height determined by electrical measurements in this work is also reported. The dashed line represents the theoretical dependence predicted by the Schottky–Mott relation.

metal/semiconductor contacts, as these measurements are not influenced by the barrier inhomogeneity and does not involve current flow through the interface [46]. Then, in Fig. 6, a collection of literature values [34, 47–49] of the Ni/AlGaN barrier height obtained by photoemission measurements is reported as a function of the Al-concentration. The experimental value of the flat-band barrier height determined by electrical measurements in this work assuming the "two diodes model" is also reported for comparison.

The dashed line represents the theoretical barrier height calculated according to the Schottky–Mott relation for Ni/AlGaN interface and considering the dependence of χ_{AlGaN} on the Al-concentration ($\Phi_{FB} = \Phi_m^{Ni} - \chi_{AlGaN} = 5.10 - (4.20 - 2.15\ x_{Al})$ eV) is also reported in this graph as a function of Al-concentration.

As can be seen, the literature photoemission data and our electrical result follow the trend predicted by the theoretical curve, thus confirming the validity of our method based on electrical analysis.

4 Conclusions The electrical behaviour of Ni/Au Schottky contacts on AlGaN/GaN heterostructures has been investigated at different temperatures. In particular, two different regions have been identified in the forward J–V characteristics of the diodes, which cannot be simply described by standard thermionic emission model. Hence, a "two diodes model" has been adopted, considering also the presence of a second barrier at the AlGaN/GaN interface in the description. A combination between forward J–V and C–V curves acquired on the Schottky contacts was used in our approach. The C–V curves allowed to take into account the influence of the Schottky contact on the 2DEG properties and hence, to correctly determine the value of the second barrier height ($\Phi_{B2}(0) = 0.28$ eV). Accordingly, the zero-bias barrier height of the Ni/AlGaN interface $\Phi_{B1}(0)$ could be calculated at each measurements temperature. The strong temperature dependence of $\Phi_{B1}(0)$ was an indication of the presence of an inhomogeneous barrier.

Therefore, the flat-band barrier height Φ_{FB} calculated at zero electric field has been introduced, which is an intrinsic property of the metal/semiconductor interface and should not depend on barrier inhomogeneities. Considering the ideality factor of our experimental curves and the properties of the used heterostructures, a value of $\Phi_{FB} = 1.40$ eV has been obtained. Such a value is closer to the theoretical one predicted by Schottky–Mott relation (1.44 eV) and followed well the expected trend of literature photoemission data for heterostructures with different Al-concentration. This latter result confirms the validity of our approach to determine the properties of the barrier height in Schottky contact fabricated on AlGaN/GaN heterostructures by electrical measurements. The method can be applied to get a fundamental understanding of the properties of the metal gates in AlGaN/GaN heterostructures and, ultimately, used to predict and optimize the performances of AlGaN/GaN HEMTs devices.

Appendix I

According to the "two diodes model," the diode D_2 is under reverse bias. Hence, the current density J_{D2} in the Reg. II can approximated in the form of a saturation current:

$$J_{D2} \approx A^* T^2 e^{-\frac{q\Phi_{B2}(V_2)}{kT}} \tag{A1}$$

where $\Phi_{B2}(V_2)$ is the barrier height seen by the carriers at the AlGaN/GaN interface, which is dependent on the voltage drop V_2 on the diode.

Considering the Reg. II of the J–V curves, that is, well below the series resistance region, the voltage-dependent barrier height $\Phi_{B2}(V_2)$ can be expanded as a first order Taylor series:

$$\Phi_{B2}(V_2) = \Phi_{B2}(0) - \left(\frac{\partial \Phi_{B2}}{\partial V_2}\right) V_2 = \Phi_{B2}(0) - \left(\frac{1}{n_2}\right) V_2 \tag{A2}$$

where $\Phi_{B2}(0)$ is the zero-bias barrier height of the diode D_2 and $\frac{\partial \Phi_{B2}}{\partial V_2}$ is the variation of the barrier Φ_{B2} with respect to the voltage drop V_2 (i.e., the inverse of the ideality factor n_2 of the diode D_2).

Substituting Eq. A2 in Eq. A1 results into the following expression for the current density of the diode D_2:

$$J_{D2} \approx A^* T^2 e^{-\frac{q\Phi_{B2}(0)}{kT}} e^{\frac{qV}{n_2 kT}} = J_{S2} e^{\frac{qV}{n_2 kT}} \tag{A3}$$

where J_{S2} is the saturation current density.

It is interesting to note that, although it has been derived for diode D_2 under reverse bias, Eq. A3 formally appears as the equation of a Schottky diode under forward bias. Hence, J_{S2} can be determined by linear fitting of the experimental forward J–V curves in the Reg. II.

Appendix II

The expression of the forward current density in a "non-ideal" diode can be written as:

$$J_D = A^* T^2 e^{-\frac{q\Phi_B(0)}{kT}} e^{\frac{qV}{nkT}} \tag{A4}$$

where n is the ideality of the diode and $\Phi_B(0)$ is the metal/semiconductor barrier height extrapolated at zero-bias.

Alternatively, the "non-ideality" of the diode can be taken into account considering the equation of an ideal diode ($n = 1$) and introducing a dependence of the Schottky barrier

on applied bias, $\Phi_B(V)$, that is:

$$J_D = A^* T^2 e^{-\frac{q\Phi_B(V)}{kT}} e^{\frac{qV}{kT}}. \tag{A5}$$

In order to determine the flat-band barrier height at zero electric field Φ_{FB}, the barrier height must be calculated at the flat-band voltage $\Phi_B(V_{FB})$.

Therefore, combining Eq. A4 and Eq. A5 at $V = V_{FB}$:

$$-\Phi_B(0) + \frac{V_{FB}}{n} = -\Phi_{FB} + V_{FB} \tag{A6}$$

For the simplest case of a Schottky contact on a n-type semiconductor, the flat-band voltage V_{FB} can be expressed as:

$$V_{FB} = \Phi_{FB} - V_n \tag{A7}$$

Then, introducing Eq. A7 in Eq. A6 allows to derive the expression of the flat-band voltage barrier height for a metal/semiconductor contact on a n-type semiconductor [40]:

$$\Phi_{FB} = n\,\Phi_B(0) - (n-1)\,V_n \tag{A8}$$

For the case of a Schottky contact on AlGaN/GaN heterostructures, an analogous procedure as the one used to derive Eq. A6 leads to the expression:

$$-\Phi_{B1}(0) + \frac{V_{FB}}{n} = -\Phi_{FB} + V_{FB} \tag{A9}$$

where $\Phi_{B1}(0)$ is the zero-bias barrier height at the metal/AlGaN interface.

In this case, the flat-band voltage V_{FB} can be expressed as:

$$V_{FB} = \Phi_{FB} - \Phi_{B2}(0) \tag{A10}$$

where $\Phi_{B2}(0)$ is the zero-bias barrier height at AlGaN/GaN interface.

Then, combining Eq. A9 with A10 allows us to determine the expression of Φ_{FB} for a Schottky contact on an AlGaN/GaN heterostructure:

$$\Phi_{FB} = n\,\Phi_{B1}(0) - (n-1)\,\Phi_{B2}(0) \tag{A11}$$

References

[1] O. Ambacher, B. Foutz, J. Smart, J. R. Shealy, N. G. Weimann, K. Chu, M. Murphy, A. J. Sierakowski, W. J. Schaff, L. F. Ea-stman, R. Dimitrov, A. Michell, and M. Stutzmann, J. Appl. Phys. **87**, 334 (2000).

[2] J. W. Chung, W. E. Hoke, E. M. Chumbes, and T. Palacios, IEEE electron dev. Lett. **31**, 195 (2010).

[3] F. Roccaforte, P. Fiorenza, G. Greco, R. Lo Nigro, F. Giannazzo, A. Patti, and M. Saggio, Phys. Status Solidi A **211**, 2063 (2014).

[4] M. Kuzuhara and H. Tokuda, IEEE Transaction on Electron Dev. **62**, 405 (2015).

[5] E. Zanoni, M. Meneghini, A. Chini, D. Marcon, and G. Mene-ghesso, IEEE Trans. Electron Dev. **60**, 3119 (2013).

[6] Y. Wu, C-Y. Chen, and J. A. del Alamo, J. Appl. Phys. **117**, 025707 (2015).

[7] J. D. Guo, F. M. Pan, M. S. Feng, R. J. Guo, P. F. Chou, and C. Y. Chang, J. Appl. Phys. **80**, 1623 (1996).

[8] T. U. Kampen and W. Mönch, Appl. Surf. Sci. **117-118**, 288 (1997).

[9] P. Hacke, T. Detchprohm, K. Hiramatsu, and N. Sawaki, Appl. Phys. Lett. **63** (2003) 2676.

[10] J. K. Kim, H. W. Jang, and J. L. Lee, J. Appl. Phys. **94**, (2003) 7201.

[11] C. Lu and S. Noor Mohammad, Appl. Phys. Lett. **89**, 162111 (2006)

[12] F. Roccaforte, F. Giannazzo, F. Iucolano, J. Eriksson, M. H. Weng, and V. Raineri, Appl. Surf. Sci. **256**, 5727–5735 (2010).

[13] L. S. Yu, Q. Z. Liu, Q. J. Xing, D. J. Qiao, S. S. Lau, and J. Re-dwing, J. Appl. Phys., **84**, 2099 (1998).

[14] J. Kotani, T. Hashizume, and H. Hasegawa, J. Vac. Sci. Technol. B **22**, 2179 (2004).

[15] A. R. Arehart, B. Moran, J. S. Speck, U. K. Mishra, S. P. DenBaars, and S. A. Ringela, J. Appl. Phys. **100**, 023709 (2006).

[16] Y. Zhou, D. Wang, C. Ahyi, C-C. Tin, J. Williams, M. Par-ka, N. M. Williams, A. Hanser, and E. A. Preble, J. Appl. Phys. **101**, 024506 (2007).

[17] Y.-J. Lin, J. Appl. Phys. **106**, 013702 (2009).

[18] Y. Wang, S. Alur, Y. Sharma, F. Tong, R. Thapa, P. Gartland, T. Issacs-Smith, C. Ahyi, J. Williams, M. Park, M. Johnson, T. Paskova, E. A. Preble, and K. R. Evans, Semicond. Sci. Technol. **26**, 022002 (2011).

[19] M. L. Lee, J. K. Sheu, and S. W. Lin, Appl. Phys. Lett. **88**, 032103 (2006).

[20] F. Iucolano, F. Roccaforte, F. Giannazzo, and V. Raineri, J. Appl. Phys. **104**, 093706 (2008).

[21] N. Miura, T. Nanjo, M. Suita, T. Oishi, Y. Abe, T. Ozeki, H. Ishikawa, T. Egawa, and T. Jimbo, Solid-State Electron. **48**, 689 (2004).

[22] K. Shiojima, T. Suemitsu, and M. Ogura, Appl. Phys. Lett. **78**, 3636 (2001).

[23] J. Spradlin, S. Dogan, J. Xie, R. Molnar, A. A. Baski, and H. Morkoc, Appl. Phys. Lett. **84**, 4150 (2004).

[24] F. Iucolano, F. Roccaforte, F. Giannazzo, and V. Raineri, J. Appl. Phys. **102**, 113701 (2007).

[25] N. Miura, T. Oishi, T. Nanjo, M. Suita, Y. Abe, T. Ozeki, H. Ishikawa, and T. Egawa, IEEE Trans. Electron Devices **51**, 297 (2004).

[26] S. T. Bradley, S. H. Goss, J. Hwang, W. J. Schaff, and L. J. Bril-lson, J. Appl. Phys. **97**, 084502 (2005).

[27] S. Saadaoui, M. Mongi Ben Salem, M. Gassoumi, H. Maa-ref, and C. Gaquie're, J. Appl. Phys. **110**, 013701 (2011).

[28] H. Zhang, E. J. Miller, and E. T. Yu, J. Appl. Phys. **99**, 023703 (2006).

[29] E. Arslan, S. Altindal, S. Özçelik, and E. Ozbay, J. Appl. Phys. **105**, 023705 (2009).

[30] D. Yan, J. Jiao, J. Ren, G. Yang, and X. Gu, J. Appl. Phys. **114**, 144511 (2013).

[31] A. F. M. Anwar, and E. W. Faraclas, Solid-State Electron. **50**, 1041 (2006).

[32] T-C. Nam, J-S. Jang, and T-Y. Seong, Curr. Appl. Phys. **12**, 1081 (2012).

[33] C. H. Chen, S. M. Baier, D. K. Arch, and M. S. Shur, IEEE Trans. Electron Devices **35**, 570 (1988).

[34] Y. Lv, Z. Lin, T. D. Corrigan, J. Zhao, Z. Cao, L. Meng, C. Luan, Z. Wang, and H. Chen, J. Appl. Phys. **109**, 074512 (2011).

[35] F. Iucolano, G. Greco, and F. Roccaforte, Appl. Phys. Lett. **103**, 201604 (2013).

[36] F. Iucolano, F. Roccaforte, F. Giannazzo, and V. Raineri, Appl. Phys. Lett. **90**, 092119 (2007).

[37] E. H. Rhoderick and R. H. Williams, Metal-Semiconductor Contacts (Oxford Science, Oxford, 1988).

[38] M. Wittmer, Phys. Rev. B **42**, 5249 (1990).

[39] M. K. Hudait and S. B. Krupanidhi, Physica B **307**, 125–137 (2001).

[40] R. T. Tung. Recent advances in Schottky barrier concepts. Mater. Sci. Eng. R, **35**, 1–138 (2001).

[41] F. Roccaforte, F. La Via, V. Raineri, R. Pierobon, and E. Zanoni, J. Appl. Phys., **93**, 9137 (2003).

[42] F. Iucolano, F. Roccaforte, F. Giannazzo, and V. Raineri, J. Appl. Phys. **102**, 113701 (2007).

[43] F. Roccaforte, F. La Via, V. Raineri, R. Pierobon, and E. Zanoni, J. Appl. Phys. **93**, 9137 (2003).

[44] G. Martin, A. Botchkarev, A. Rockett, and H. Morkoç, Appl. Phys. Lett. **68**, 2541 (1996).

[45] L. F. Wagner, R. W. Young, and A. Sugerman, IEEE Electron Device Lett. **4**(9), 320 (1983).

[46] D. K. Schroder, Semiconductors Materials and Device Characterization, 3rd ed. (John Wiley & Sons, New York, 2006).

[47] L. S. Yu, Q. J. Xing, D. Qiao, S. S. Lau, K. S. Boutros, and J. M. Redwing, Appl. Phys. Lett. **73**, 3917 (1998).

[48] D. Qiao, L. S. Yu, S. S. Lau, J. M. Redwing, J. Y. Lin, and H. X. Jiang, J Appl. Phys. **87**, 2 (2000).

[49] A. R. Arehart, A. A. Allerman, and S. A. Ringel, J Appl. Phys. **109**, 114506 (2011).